Research Article | Vol. 26, No. 20 | 1 Oct 2018 | OPTICS EXPRESS 25761
Optics EXPRESS

Few-mode fiber true time delay lines for distributed radiofrequency signal processing

RUBÉN GUILLEM,* SERGI GARCÍA, JAVIER MADRIGAL, DAVID BARRERA, AND IVANA GASULLA

ITEAM Research Institute, Universitat Politècnica de València, Camino de Vera 46022 Valencia, Spain
**ruguico@iteam.upv.es*

Abstract: We report, for the first time to our knowledge, distributed radiofrequency signal processing built upon true time delay operation on a step-index few-mode fiber. Two 3-sample configurations with different time delay properties are implemented over the same 60-meter 4-LP-mode fiber link. The inscription of a long period grating at a specific fiber position converts part of the LP_{01} mode into the LP_{02}, permitting sample time delay engineering. Delay line performance is experimentally demonstrated when applied to radiofrequency signal filtering, example of fiber-distributed processing functionality exhibiting one order or magnitude gain in terms of compactness.

1. Introduction

Space-division multiplexing (SDM) optical fibers [1] not only can provide parallel signal distribution but also exhibit great potential for distributed signal processing, concept that agglutinates both parallel signal processing and delivery functionalities over the same single optical fiber. Such a performance is particularly attractive to short- and medium-reach fiber-wireless scenarios that must provide some kind of radiofrequency (RF) signal processing, as the case of radio access networks for 5G communications. But it also extends to a broad range of fields where photonic signal processing is required, such as medical imaging, autonomous driving and communication as well as high-resolution sensing.

Distributed signal processing has been previously proposed and demonstrated using multicore fibers (MCFs) [2], including both multicavity devices based on the selective inscription of fiber Bragg gratings in homogeneous MCFs [3], and dispersion-engineered heterogeneous MCF links up to a few km, [4]. The latter implies the customization of each fiber core to provide specific spectral group delay characteristics in a way that every core transport a given sample of the RF signal with the specific time delay required for true time delay line (TTDL) operation. Sampled TTDLs are indeed the basis of most Microwave Photonics (MWP) incoherent signal processing functionalities [5], such as microwave signal filtering, optoelectronic oscillation, optical beamforming for phased-array antennas or arbitrary waveform generation. Distributed signal processing can also be developed over short-reach few-mode fiber (FMF) links, where one needs to engineer the fiber so that every mode (or, to be more precise, every group of modes) experiences, at a given optical wavelength, the adequate group delay to fulfil the main principle for TTDL operation, that is, a constant differential time delay between adjacent samples (named as basic differential delay). We must assure, in addition, a low level of coupling between groups of modes, what calls for the predilection of refractive step-index (SI) profiles and the use of short distances combined with direct detection techniques. Actually, RF signal processing built upon FMF links may be preferred for covering distances lower than 1 km (as is the case in in-home or in-building scenarios), while MCFs will be more suitable for links reaching up to a few km (for instance, connecting central offices and base stations in radio access networks). When comparing both SDM fibers, we must bear in mind as well that, in general, the fabrication process is more complex and expensive in the case of MCFs.

#340975 https://doi.org/10.1364/OE.26.025761
Journal © 2018 Received 1 Aug 2018; revised 12 Sep 2018; accepted 13 Sep 2018; published 18 Sep 2018

Optics EXPRESS

In this paper, we propose and experimentally demonstrate, for the first time to our knowledge, sampled TTDL operation with constant basic differential delay along a SI FMF. Two different TTDLs, which are characterized by different basic differential delays, are implemented over the same 60-m FMF that propagates 4 LP modes (LP_{01}, LP_{11}, LP_{21} and LP_{02}). A long period grating (LPG) inscribed at a specific position along the fiber allows the modification of the time delay of the sample linked to the LP_{02} mode. Delay line selection is realized by choosing a proper set of 3 modes at the fiber output. As a proof of concept, we apply the implemented sampled TTDL to a typical RF signal processing functionality, RF signal filtering, obtaining a good agreement between theoretical and experimental results.

2. True time delay line operation based on a few-mode fiber

We propose to implement sampled TTDL operation on a step-index FMF, provided by Prysmian, which supports four LP modes (LP_{01}, LP_{11}, LP_{21} and LP_{02}). The fiber is characterized by a 15-μm core diameter, a 125-μm cladding diameter and a refractive index contrast of 1.1%. At a wavelength of 1550 nm, the differential group delays (DGDs) relative to LP_{01} mode are 4.4, 8.9 and 7.9 ps/m, respectively for LP_{11}, LP_{21} and LP_{02} modes, and the chromatic dispersion values are 21, 26, 19 and 8 ps/km/nm, respectively for LP_{01}, LP_{11}, LP_{21} and LP_{02} modes, [6]. The group delay per unit length τ_n for a fiber mode n can be expanded as a first-order Taylor series [4] around an anchor wavelength λ_0 as:

$$\tau_n(\lambda) = \tau_n(\lambda_0) + D_n(\lambda_0)(\lambda - \lambda_0), \quad n = \{01, 11, 21, 02\}, \tag{1}$$

where D_n is the chromatic dispersion parameter of mode n at λ_0. Higher-order dispersion effects are assumed to be similar in all mode groups and, therefore, can be neglected in terms of DGD calculation. Sampled TTDL operability requires identical basic differential delays between adjacent samples Δt, [5]. From the above fiber group delay and dispersion specifications, we see that the first three modes (i.e., modes LP_{01}, LP_{11} and LP_{21}) almost satisfy this condition, and thus one can expect that it will occur at some point nearby 1550 nm. By solving the equation system formed by Eq. (1) for these modes, we found that the wavelength λ_T = 1558.3 nm forces the DGD between LP_{21} and LP_{01} modes to double the DGD between LP_{11} and LP_{01} modes. If the first, second and third samples correspond, respectively, to the LP_{01}, LP_{11} and LP_{21} modes, then the total time delay of the samples t_k (where k = 1, 2, 3) fulfil:

$$t_3 - t_1 = 2(t_2 - t_1). \tag{2}$$

As illustrated in Fig. 1(b), one can find, for any fiber length, three equally temporary spaced optical samples when operating at the optical wavelength λ_T. The processing radiofrequency depends on the inverse of the basic differential delay Δt, which is determined by the fiber length. As further described in section 4, a fiber length of L = 60 m leads to Δt_1 = 285.7 ps, so that the processing radiofrequency falls within the frequency range of our measurement system.

We must take into account that we cannot implement a 4-sample TTDL with all the propagating modes since the LP_{02} mode does not fulfil the constant basic differential delay condition. Therefore, we use this mode for implementing, at the same time, another 3-sample delay line in a way that one can manually switch between the two delay lines by simply changing the set of modes extracted at the output of the FMF link.

The first, second and third samples featuring this second delay line will be given, respectively, by LP_{01}, LP_{02} and LP_{11} modes at the fiber output as long as we assure a constant basic differential delay. To achieve this, we propose to realize a mode conversion by the inscription of an LPG at a specific longitudinal position along the fiber so that the total delay of one sample is modified accordingly. Figure 1(a) illustrates this concept. Since each mode is characterized by a different group delay, the new sample's delay will then be determined by a ponderation between the group delays of both modes involved. In our case, the time delay of

Optics EXPRESS

the second sample is adjusted by combining the propagation characteristics of the LP_{01} and LP_{02} modes. This sample will propagate firstly through LP_{01} along a certain distance L' of the FMF link. At this point, part of the energy propagating through LP_{01} will couple to LP_{02} mode. This second sample will then propagate through LP_{02} mode along the remaining distance $L - L'$, as shown in Fig. 1(a). The time delay of the first and third samples are obtained, respectively, from the modal groups delays as $t_1 = \tau_{01}L$ and $t_2 = \tau_{11}L$. For the second sample, the total time delay t_2 is given by:

$$t_2 = L'\left[\tau_{01} + D_{01}\left(\lambda - \lambda_0\right)\right] + (L - L')\left[\tau_{02} + D_{02}\left(\lambda - \lambda_0\right)\right]. \quad (3)$$

Equations (2) and (3) yield $L' = 0.285L$ for $\lambda = 1558.3$ nm. Thus, by introducing the LPG at 0.285 times the total length, TTDL operation is possible for the second set of three fiber modes, as shown in Fig. 1(b) lower. In particular, for a fiber link length of 60 m, the LPG must be placed at the position $L' = 17.1$ m and the TTDL basic differential delay is $\Delta t_2 = 137$ ps.

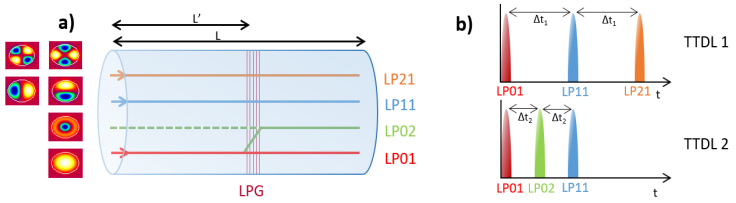

Fig. 1. Sampled true time delay line operation over a few-mode fiber. a) Scheme of the FMF link of length L with an LPG inscribed at the position L' to excite the LP_{02} mode. b) Optical samples in the time domain for the two possible TTDL schemes characterized by different basic differential delays Δt.

As mentioned before, we will evaluate the performance of both TTDLs when they are applied to three-tap RF photonic filtering. By choosing a given set of samples, (either the ones extracted from $LP_{01,}$ LP_{11} and LP_{21} modes, or those extracted from $LP_{01,}$ LP_{02} and LP_{11} modes at the FMF output), we can select a different microwave photonic filter.

3. Long period grating inscription

With grating periods Λ typically ranging from 100 μm up to 1 mm, LPGs can induce coupling from a propagating core mode to another forward-propagating core mode if the grating period equals the beat length of the modes. This energy transfer takes place at the central wavelength of the LPG that depends on the period Λ and the difference between the effective refractive indices of the modes [7]. In our case, for mode conversion between LP_{01} and LP_{02}, we have:

$$\lambda = \Lambda(n_{eff_{LP01}} - n_{eff_{LP02}}). \quad (4)$$

LPGs have found application in band rejection filters [8], gain flattering filters [9], temperature sensors [10], curvature sensors [11], refractive index sensors [12], and mode conversion in FMFs [13]. They are low loss and have low reflection and high design flexibility. They can be created either as a mechanical perturbation over the fiber or inscribed as a permanent perturbation with a UV laser.

We inscribed the LPG with direct point-by-point UV laser inscription. Prior to the inscription, the FMF was hydrogen-loaded at ambient temperature for two weeks at a pressure of 50 bar to increase its photosensitivity. The grating was inscribed with a frequency-doubled argon-ion laser emitting at 244 nm, with an output power of 50 mW and an exposure time of 20 s. Photonic lanterns were spliced at both ends in order to monitor the optical output powers of all modes during the inscription. The inscribed period was 263 μm, which was selected to get the mode change at 1550-nm wavelength for the Prysmian fiber, while the LPG length was set to 29 mm to achieve the complete mode change. After the inscription, a heat

Optics EXPRESS

annealing was done to assure the stabilization of the LPG by heating the fiber up to 200 °C for five hours and thus accelerating the degradation effects associated with the hydrogen diffusion and the refractive index thermal decay. Prior to heat annealing, we observed both short-time and long-time variations, due to the hydrogen content. Short-time variations are produced after inscription when hydrogen is redistributed from non-affected sections of fiber to irradiated sections where the grating is inscribed, and long-time variations are produced when hydrogen leaks out of the fiber [8,14,15].

Figure 2(a) shows the optical spectra for the two modes 16 hours after the inscription. Spectrum deformations can be observed at the mode-conversion wavelength due to energy leaking from LP_{02} mode to higher-order cladding modes. After five hours of heat annealing, the optical spectrum is properly recovered and an efficient mode conversion between LP_{01} and LP_{02} modes is achieved and maintained over time at a wavelength of 1550 nm (see Fig. 2(b)). The output power of both modes can be controlled by tuning the wavelength in the vicinity of the LPG response. In particular, we are interested in working at 1558.3 nm, where the conversion efficiency of the LPG translates into output optical powers of −4.8 and −2.2 dB, respectively, for LP_{01} and LP_{02} modes. The three samples of the delay line are then obtained, at the output of the fiber, as the upcoming signals from: (1) the remaining power at LP_{01} mode; (2) the generated LP_{02} mode; and (3) the LP_{11} mode.

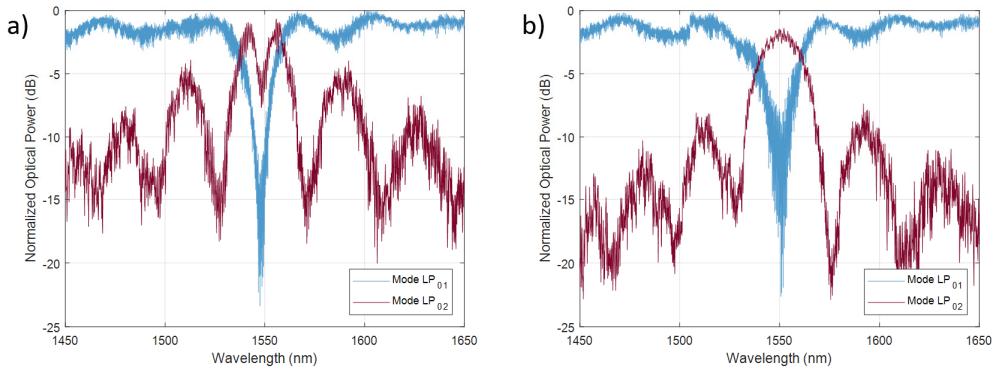

Fig. 2. Measured optical spectral response of the inscribed LPG for modes LP_{01} and LP_{02}, (a) 16 hours after inscription and (b) after 5 hours of heat annealing.

4. Experimental demonstration and application to RF photonic signal filtering

Figure 3 shows the experimental setup for RF signal filtering assembled with the implemented TTDL. We use a laser emitting at 1558.3 nm, an external electro-optic intensity modulator, a photodetector and a vector network analyzer (VNA). After the modulator, the light is split in three paths and injected into the FMF using a photonic lantern [16], so that the modes LP_{01}, LP_{11} and LP_{21} are excited. After the FMF link, the signals propagated by the four LP modes are recovered using the second photonic lantern. The photonics lanterns were fabricated by Olkin Optics explicitly for the Prysmian FMF [17]. We characterized their performance by measuring the insertion losses (gathered in Table 1) and the average intermodal crosstalk between modes at 1550 nm (gathered in Table 2) when both photonic lanterns are connected directly. One can observe that the insertion losses are not constant due to several phenomena that affect each mode differently, as fiber offset induced splice misalignments and possible manufacturer errors. We can see in addition higher levels of crosstalk for any mode coupling combination that involves the LP_{11} mode, what may have important repercussions on the overall behavior of the system. In general, the effect of modal crosstalk must be carefully tackled since it can degrade the response of the microwave photonic filter.

Optics EXPRESS

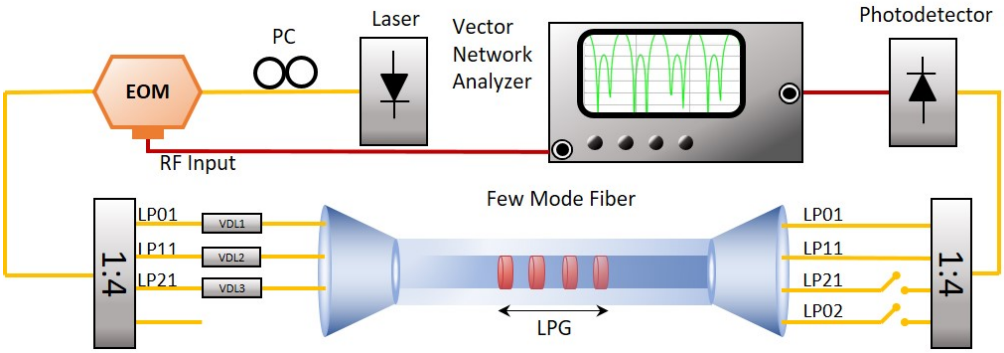

Fig. 3. Experimental setup for RF filtering implemented with the developed FMF-based true time delay line. EOM: electro-optic modulator, PC: polarization controller, VDL: variable delay line, LPG: long period grating.

Table 1. Measured insertion losses for both photonic lanterns at 1550 nm.

Insertion Losses (dB)	
LP_{01}	–3.68
LP_{11}	–5.20
LP_{21}	–5.83
LP_{02}	–7.18

Table 2. Measured intermodal crosstalk (dB) for both photonic lanterns at 1550 nm.

	LP_{01} out	LP_{11} out	LP_{21} out	LP_{02} out
LP_{01} in	N/A	–12.44	–24.05	–26.9
LP_{11} in	–14.45	N/A	–15.60	–13.75
LP_{21} in	–20.86	–12.74	N/A	–18.56
LP_{02} in	–24.70	–15.09	–17.83	N/A

At the output of the photonic lantern, we can choose between the two possible signal filters by selecting the appropriate set of modes. We must take into account that the RF filter must arise from the TTDL implemented by the FMF itself, so we compensated any other influence over the group delay introduced by external components by adjusting three variable delay lines (VDLs) introduced before the FMF. The basic differential delay between samples was therefore adjusted to zero when the FMF was not present in the system. We have measured the differential delay of each mode by using an interferometric-based technique [18], which allows us to compensate the setup with a precision of 2 ps.

The basic differential delays of both TTDL schemes (i.e., $\Delta t_1 = 285.7$ and $\Delta t_2 = 137.0$ ps), generate microwave photonic filters with expected free spectral ranges (FSRs) of 3.75 and 7.50 GHz, respectively. These FSR values allow us to measure multiple filter resonances in the vector network analyzer.

We work only with the spatial LP_{lma} modes to avoid any additional system required to combine the *a* and *b* spatial field components. In the context of SDM distribution of parallel channels, the signals propagated through degenerate modes should be in principle combined using an optical or electrical diversity combiner stage before or after photodetection if direct detection is used, [19]. The application of these techniques to MWP signal processing must be further investigated since (1) the use of electrical diversity combining is not compatible, for instance, with RF signal filtering where all the samples must be combined optically before detection, and (2) the use of optical combining requires applying adaptive co-phasing before adding both modes together in the optical domain that will significantly increase the complexity of the system.

Optics EXPRESS

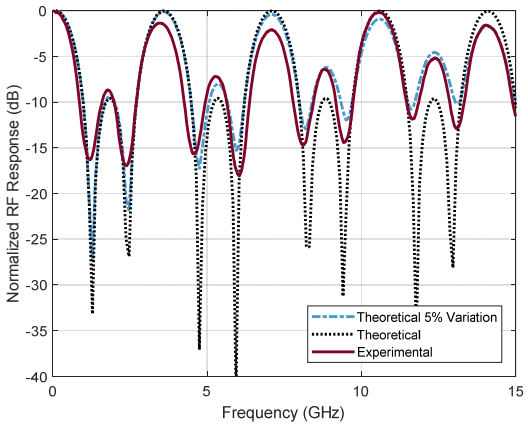

Fig. 4. Normalized radiofrequency response of the RF filter implemented with the first set of modes: LP_{01}, LP_{11a} and LP_{21a}. Blue dashed line: theoretical results with 5% time-periodicity variation; black dotted line: theoretical ideal results; maroon solid line: experimental results.

Figure 4 shows the normalized radiofrequency response of the microwave photonic filter implemented with the first TTDL, which is given by the set of modes LP_{01}, LP_{11a} and LP_{21a}. The maroon solid line corresponds to the experimental result, while the black dotted line corresponds to the theoretical result for an ideal uniform three-tap filter, obtained as the time-to-frequency Fourier transform of three Gaussian samples spaced 285.7 ps. We can see that the theoretical and experimental results agree very well in terms of frequency periodicity, but there exists some degradation for increasing frequencies in terms of main-to-secondary sidelobe ratio. This degradation may be caused mainly by small variations in the differential delay between adjacent samples. Hence, we computed the frequency response where the time periodicity of the samples is varied a 5% around the theoretical Δt value, that is, a 7-ps variation (blue dashed line). As observed, this adjustment leads to a better agreement for high frequencies. This time variation can be understood as an accumulation of precision errors. Actually, the systematic error of our setup for the time delay measurement of one sample is 2 ps. The 7-ps time deviation corresponds to 3.5 times this systematic error, which falls close to the measurement uncertainty we can expect.

Additional effects that might contribute to the time delay variation include: (1) fluctuations in the groups delays of the FMF modes that arise from variations in the laboratory environmental conditions; (2) mismatching between the modal DGD values provided in the FMF specifications and the actual values, what in addition translates into a deviation from both the theoretical optimal wavelength λ_T and the longitudinal position of the LPG along the fiber L'; and (3) slight variations in the fiber lengths L and L' due to fiber cutting imprecision.

Furthermore, we must take into account that the intermodal crosstalk arisen in both the FMF link and the photonic lanterns introduces some distortion in the RF frequency response as the amplitude windowing of the time samples is altered. In particular, the central TTDL sample, which is carried by the LP_{11} mode, is the one contributing the most to this effect, as corroborated by Table 2.

Optics EXPRESS

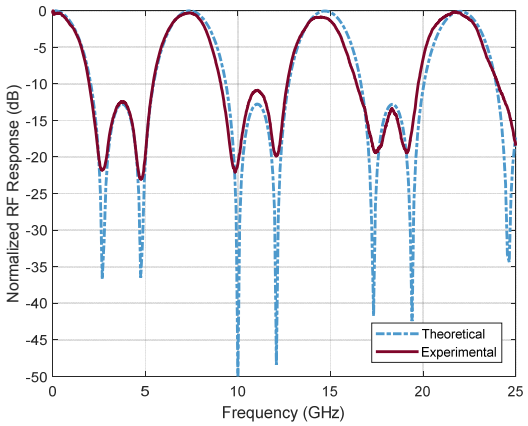

Fig. 5. Normalized radiofrequency response of the RF filter implemented with the second set of modes: LP_{01}, LP_{02} and LP_{11a}. Blue dashed blue line: theoretical results; maroon solid line: experimental results.

Figure 5 illustrates the normalized radiofrequency response of the microwave photonic filter implemented with the second TTDL, which is produced by the set of modes LP_{01}, LP_{02} and LP_{11a}. The maroon solid line corresponds to the experimental results while the blue dashed line represents the theoretical response for an ideal apodized three-tap filter, obtained as the time-to-frequency Fourier transform of three Gaussian samples, where the power of central tap is 20% higher than the rest and the basic differential delay is Δt_2 = 137 ps. As we can see, the experimental results show a very good agreement with the apodized theoretical simulation. The different attenuation level introduced by the LPG at 1558.3 nm, which is –4.8 dB for LP_{01} mode and –2.2 dB for LP_{02} mode (as shown in Fig. 2(b)), is the main responsible for this amplitude apodization.

5. Conclusions

We have proposed and experimentally demonstrated the first parallel TTDL for RF signals developed on a few-mode fiber link, where the 4 LP modes act as the optical carriers for the delay line samples. The introduction of an LPG to partially transform the LP_{01} mode into the LP_{02} mode at the proper link distance enables participation of the LP_{02} mode in the TDDL operation. Two different configurations with different time delay properties are implemented on the same fiber, both ensuring a constant differential delay between samples, which is an essential requirement for incoherent discrete-time signal processing. The performance of the TTDL has been evaluated in the context of microwave signal filtering where we successfully demonstrated two filters where the FSR depends on the set of modes recovered.

This work demonstrates the feasible implementation of parallel distributed signal processing along a single FMF without resorting to parallel singlemode fiber links. This solution can be applied to a variety of MWP functionalities that will especially demanded in next-generation fiber-wireless communications, including not only signal filtering but also optical beamforming in phased-array antennas and arbitrary waveform generation among others.

Funding

H2020 European Research Council (ERC) (Consolidator Grant 724663); Spanish MINECO (TEC2014-60378-C2-1-R and TEC2016-80150-R projects, BES-2015-073359 scholarship for S. García, Ramon y Cajal fellowship RYC-2014-16247 for I. Gasulla).

Optics EXPRESS

Acknowledgments

We thank Prysmian for providing the FMF.

References

1. D. J. Richardson, J. M. Fini, and L. E. Nelson, "Space-division multiplexing in optical fibers," Nat. Photonics **7**(5), 354–362 (2013).
2. I. Gasulla and J. Capmany, "Microwave photonics applications of multicore fibers," IEEE Photonics J. **4**(3), 877–887 (2012).
3. I. Gasulla, D. Barrera, J. Hervás, and S. Sales, "Spatial division multiplexed microwave signal processing by selective grating inscription in homogeneous multicore fibers," Sci. Rep. **7**(1), 41727 (2017).
4. S. García and I. Gasulla, "Dispersion-engineered multicore fibers for distributed radiofrequency signal processing," Opt. Express **24**(18), 20641–20654 (2016).
5. J. Capmany, J. Mora, I. Gasulla, J. Sancho, J. Lloret, and S. Sales, "Microwave photonic signal procesing," J. Lightwave Technol. **31**(4), 571–586 (2013).
6. H. Wen, Q. Mo, P. Sillard, R. A. Correa, and G. Li, "Analog transmission over few-mode fibers," in *Optical Fiber Communication Conference*, OSA Technical Digest (online) (Optical Society of America, 2016), paper Th4A.3.
7. V. Bhatia and A. M. Vengsarkar, "Optical fiber long-period grating sensors," Opt. Lett. **21**(9), 692–694 (1996).
8. A. M. Vengsarkar, P. J. Lemaire, J. B. Judkins, V. Bhatia, T. Erdogan, and J. E. Sipe, "Long-period fiber gratings as band-rejection filters," J. Lightwave Technol. **14**(1), 58–64 (1996).
9. A. M. Vengsarkar, J. R. Pedrazzani, J. B. Judkins, P. J. Lemaire, N. S. Bergano, and C. R. Davidson, "Long-period fiber-grating-based gain equalizers," Opt. Lett. **21**(5), 336–338 (1996).
10. L. Madhavan, M. Chattopadhyay, "Temperature and strain sensitivity of long period grating fiber sensor: review," Int. J. Res. Eng. Technol. **4**(2), 776–782 (2015).
11. D. Barrera, J. Madrigal, and S. Sales, "Long period gratings in multicore optical fibers for directional curvature sensor implementation," J. Lightwave Technol. **36**(4), 1063–1068 (2018).
12. H. Patrick, A. Kersey, and F. Bucholtz, "Analysis of the response of long period fiber gratings to external index of refraction," J. Lightwave Technol. **16**(9), 1606–1612 (1998).
13. Y. Zhao, Y. Liu, L. Zhang, C. Zhang, J. Wen, and T. Wang, "Mode converter based on the long-period fiber gratings written in the two-mode fiber," Opt. Express **24**(6), 6186–6195 (2016).
14. G. Bai, T. Hwa, H. Siu, L. Shun, and D. Xiao, "Growth of long-period gratings in H2-loaded fiber after 193-nm UV inscription," IEEE Photonics Technol. Lett. **12**(6), 642–644 (2000).
15. S. W. James and R. P. Tatam, "Optical fibre long-period gratings sensor characteristics and application," Meas. Sci. Technol. **14**, 46–61 (2003).
16. T. A. Birks, I. G. Sánchez, S. Yerolatsitis, S. G. Leon, and R. R. Thomson, "The photonic lantern," Adv. Opt. Photonics **7**(2), 107–167 (2015).
17. A. M. Velázquez, J. Alvarado, G. Lopez, A. Schülzgen, D. Ras, P. Sillard, C. Okonkwo, and R. A. Correa, "Six spatial modes photonic lanterns," in *Optical Fiber Communication Conference*, OSA Technical Digest (online) (Optical Society of America, 2015), paper W3B.3.
18. C. Dorrer, N. Belabas, J. Linkforman, and M. Joffre, "Spectral resolution and sampling issues in Fourier-transform spectral interferometry," J. Opt. Soc. Am. B **17**(10), 1795–1802 (2000).
19. I. Gasulla and J. M. Kahn, "Performance of direct-detection mode-group-division multiplexing using fussed fiber couplers," IEEE J. Lightwave Technol. **33**(9), 1748–1760 (2015).